Neuroscience 153 (2008) 1354–1369

SELF-ORGANIZATION AND NEURONAL AVALANCHES IN NETWORKS OF DISSOCIATED CORTICAL NEURONS

V. PASQUALE,[a] P. MASSOBRIO,[b] L. L. BOLOGNA,[a] M. CHIAPPALONE[a] AND S. MARTINOIA[b]*

[a]*Neuroscience and Brain Technology Department, Italian Institute of Technology, Via Morego 30, 16163 Genova, Italy*

[b]*Neuroengineering and Bio-nano Technology Group, Department of Biophysical and Electronic Engineering, University of Genova, Via all'Opera Pia 11A, 16145 Genova, Italy*

Abstract—Dissociated cortical neurons from rat embryos cultured onto micro-electrode arrays exhibit characteristic patterns of electrophysiological activity, ranging from isolated spikes in the first days of development to highly synchronized bursts after 3–4 weeks *in vitro*. In this work we analyzed these features by considering the approach proposed by the self-organized criticality theory: we found that networks of dissociated cortical neurons also generate spontaneous events of spreading activity, previously observed in cortical slices, in the form of *neuronal avalanches*. Choosing an appropriate time scale of observation to detect such neuronal avalanches, we studied the dynamics by considering the spontaneous activity during acute recordings in mature cultures and following the development of the network. We observed different behaviors, i.e. sub-critical, critical or super-critical distributions of avalanche sizes and durations, depending on both the age and the development of cultures. In order to clarify this variability, neuronal avalanches were correlated with other statistical parameters describing the global activity of the network. Criticality was found in correspondence to medium synchronization among bursts and high ratio between bursting and spiking activity. Then, the action of specific drugs affecting global bursting dynamics (i.e. acetylcholine and bicuculline) was investigated to confirm the correlation between criticality and regulated balance between synchronization and variability in the bursting activity. Finally, a computational model of neuronal network was developed in order to interpret the experimental results and understand which parameters (e.g. connectivity, excitability) influence the distribution of avalanches.

In summary, cortical neurons preserve their capability to self-organize in an effective network even when dissociated and cultured *in vitro*. The distribution of avalanche features seems to be critical in those cultures displaying medium synchronization among bursts and poor random spiking activity, as confirmed by chemical manipulation experiments and modeling studies.

*Corresponding author. Tel: +39-010-353-2251; fax: +39-010-353-2133.
E-mail address: sergio.martinoia@unige.it (S. Martinoia).
Abbreviations: ACh, acetylcholine; AE, all electrodes shuffling; BIC, bicuculline; CI_0, coincidence index; DIV, days *in vitro*; IBI, interburst interval; IED, interelectrode distance; IEI, interevent interval; ISI, interspike interval; LFP, local field potential; MBR, mean bursting rate; MEA, micro-electrode array; RMSE, root mean squared error; SE, single electrode shuffling.

Key words: self-organized criticality, micro-electrode arrays, rat cortical neurons, *in vitro* development, scale-free network model.

Large random cortical networks developing *in vitro* and chronically coupled to micro-electrode arrays (MEAs) represent a valuable experimental model for studying the universal mechanisms governing the formation and conservation of neuronal cell assemblies (Marom and Shahaf, 2002). This preparation, unlike other experimental models such as acute and cultured cortical slices, is relatively free of predefined constraints and allows neurons to self-organize during development, creating a network that exhibits complex spatio-temporal patterns of activity (van Pelt et al., 2004a; Wagenaar et al., 2006a; Rolston et al., 2007).

Using this experimental framework, it is interesting to study how the spontaneous electrophysiological activity of the network changes and matures during development (van Pelt et al., 2005; Chiappalone et al., 2006a; Wagenaar et al., 2006b). A marked sensitiveness of the spatio-temporal firing patterns to structural changes in the network during the *in vitro* maturation has been extensively demonstrated, showing variations in the burst patterns and also in the cross-correlation among all pairs of electrodes. Mature cultures (between 21 and 35 days *in vitro* (DIV)) exhibit a synchronized and distributed bursting activity, mixed to a highly variable spiking activity. This network state has been associated to a stable condition of maturation of the culture, and synchronized bursting events have been named "network bursts" (van Pelt et al., 2004b, 2005).

Periods of synchronized electrophysiological activity are also present in other experimental models, such as acute and cultured cortical slices (Beggs and Plenz, 2003, 2004), where it has been demonstrated that within these synchronous epochs there exists a more sophisticated embedded form of dynamics, called *neuronal avalanche*. The presence of such neuronal avalanches, as an evidence of self-organized critical dynamics, has been often associated to the capability of the network to enhance the information transmission (Beggs and Plenz, 2003; Plenz and Thiagarajan, 2007). In other words, if a critical self-organization allows improvement of the transfer of information among cell assemblies, cultured systems should likely display a spontaneous tendency to move toward a critical state characterized by neuronal avalanches.

In our work, while trying to understand the phenomenon of self-organization in dissociated cortical networks, we asked whether and how neuronal avalanches are intrinsic to the network formation and stabilization. In what

0306-4522/08$32.00+0.00
doi:10.1016/j.neuroscience.2008.03.050

follows, we show that such critical states are found at a specific temporal resolution and they spontaneously appear in some cultures during the network development. Then, we describe in detail the analysis performed and the specific experiments devoted to clarify the variability of such dynamic organization. Finally, we introduce a computational model developed to interpret the experimental results and to demonstrate that networks showing spiking and bursting activity, similar to that observed in cultures of dissociated neurons, are able to reproduce neuronal avalanches at the spike-level with a power law distribution.

EXPERIMENTAL PROCEDURES

Cell culture technique

Dissociated neuronal cultures were obtained from cerebral cortices of embryonic rats, at gestational day 18. The embryos were delivered by cesarean section from deeply anesthetized rats and killed by decapitation. All experiments were carried out in accordance with the European Community Council Directive of November 24th 1986 (86/609/EEC) for the care and use of laboratory animals and approved by MIUR (Ministero dell'Universita' e Ricerca Scientifica). All efforts were made to minimize the number of animals used and their suffering.

The cerebral cortices of four to five rat embryos were chopped into small pieces and exposed to a 0.125% trypsin solution for 25–30 min at 37 °C. Then, they were mechanically dissociated by trituration through fine-tipped pipettes. The resulting tissue was resuspended in 10 ml Neurobasal medium (purchased from Invitrogen, Carlsbad, CA, USA) supplemented with 2% B27 (Brewer et al., 1993; Brewer, 1997) and 1% Glutamax-I (both Invitrogen) and diluted at the final concentration of 800,000 cells/ml. No antimitotic drug was added to prevent glia proliferation, since glial cells are known to be fundamental for the healthy development of neuronal populations (Nedergaard, 1994; Pfrieger and Barres, 1997; Araque et al., 1999). Cells were then plated on 60-channel MEAs, precoated with adhesion promoting molecules (poly-D-lysine and laminin), at the final density of $5–8\times10^4$ cells/device (Fig. 1A). They were maintained in culture dishes, each containing 1 ml of nutrient medium (i.e. serum-free Neurobasal medium supplemented with B27 and Glutamax-I) and placed in a humidified incubator having an atmosphere of 5% CO_2 and 95% O_2 at 37 °C. Half of the medium was changed weekly. Under these environmental conditions, cortical neurons showed excellent growth and robust synaptic connections that allowed us to record spontaneous electrical activity from 7 DIV up to 5–6 weeks *in vitro*.

MEAs and experimental setup

Primary cultures of cortical neurons were plated over arrays (MEA 1060, Multi Channel Systems, Reutlingen, Germany) of 60 planar TiN/SiN micro-electrodes (30 μm diameter, 200 μm spaced) and kept alive in healthy conditions for several weeks.

The experimental setup is based on the MEA 60 system, consisting of a MEA, a mounting support with integrated 60 channels pre- and filter amplifier (MEA 1060, gain 1200×) and a personal computer equipped with a PCI data acquisition board for real time signal monitoring and recording. Commercial software, MC-Rack (Multi Channel Systems), was used for on-line visualization and raw data storage; then, data were processed by using specifically developed software tools as described in the next sections.

Experimental protocols

In order to detect the presence of neuronal avalanches, we considered different experimental conditions. Unless differently specified, each culture was tested after a period of rest, to allow for a stabilization of the network out of the incubator (Streit et al., 2001). The MEA device was maintained at 37 °C to avoid temperature shock out of the incubator and to preserve the metabolic kinetics of neurotransmission. Neuronal networks were kept in the culture medium during recording and electrophysiological signals were acquired at a sampling rate of 10 kHz.

Recordings during development. Spontaneous electrophysiological activity was recorded twice a week in six cultures starting from 7 DIV until 42 DIV. Every experimental session lasted 30 min.

Considering that cultures of dissociated cortical neurons reach a stable state of maturation after the 3rd week *in vitro* (Chiappalone et al., 2006a), we focused our attention on recordings from 21 to 42 DIV, although we also applied the avalanche analysis to the earlier stage of maturation.

Acute long-lasting recordings. Long-lasting recordings were performed on three cultures, obtained from different cell preparations, during the 4th week *in vitro* (25–28 DIV). Two cultures were recorded at a sampling rate of 10 kHz, whereas the last one was recorded both at 10 and 25 kHz. All recordings lasted 1 h.

The aim of these experiments was to expand our dataset in the key period of development (i.e. 4th week *in vitro*), and test how the acquisition parameters (e.g. sampling rate, duration) could affect avalanche analysis results.

Chemical stimulation experiments. Some cultures were treated with specific drugs affecting the bursting dynamics of *in vitro* cortical networks: we tested acetylcholine (ACh) in concentration 10 μM (Gross et al., 1995) on three cultures and bicuculline (BIC) in concentration 30 μM (Keefer et al., 2001; Lin et al., 2002; Gramowski et al., 2004) on other three cultures. All agents were purchased from Sigma Aldrich (St. Louis, MO, USA).

All the experiments started with a 20-min recording of the network spontaneous activity in physiological solution (NaCl 150 mM, KCl 2.8 mM, $CaCl_2$ 1.3 mM, $MgCl_2$ 0.7 mM, Hepes 10 mM, glucose 10 mM, pH 7.3), followed by 20 min under drug treatment. The aim of these experiments was to study whether and how chemical stimulation could affect network behavior and change avalanche dynamics.

Spike detection

Extracellularly recorded signals are embedded in biological and thermal noise (Fig. 1B) and spikes can be detected using a threshold-based detection algorithm (Perkel et al., 1967; Gross et al., 1995). A previously developed ad hoc algorithm (Chiappalone et al., 2003) calculates the peak-to-peak thresholds as multiple of the standard deviation (8×S.D.) of the baseline noise (Jimbo et al., 1999) for each electrode during the spontaneous activity phase (20.7 ± 0.8 μV, mean±S.D., one culture). In this study, no attempt was made to discriminate and sort the collected spikes (Eytan and Marom, 2006).

Burst detection

Developing cortical networks show spiking activity as well as bursting behavior (Robinson et al., 1993; Opitz et al., 2002). A population burst consists of episodes of activity occurring simultaneously at many channels, spread over the entire network (Fig. 1C). The spikes belonging to a burst are time-spaced in a range of a few milliseconds; these packages generally last from hundreds of milliseconds up to seconds with long quiescent periods. Bursts were identified and their features saved (i.e. duration, rate, etc.) according to a method previously presented in the literature (Chiappalone et al., 2005). Moreover, burst event trains, containing the sequence of the initial spike of each burst (Cozzi et al., 2006), were stored.

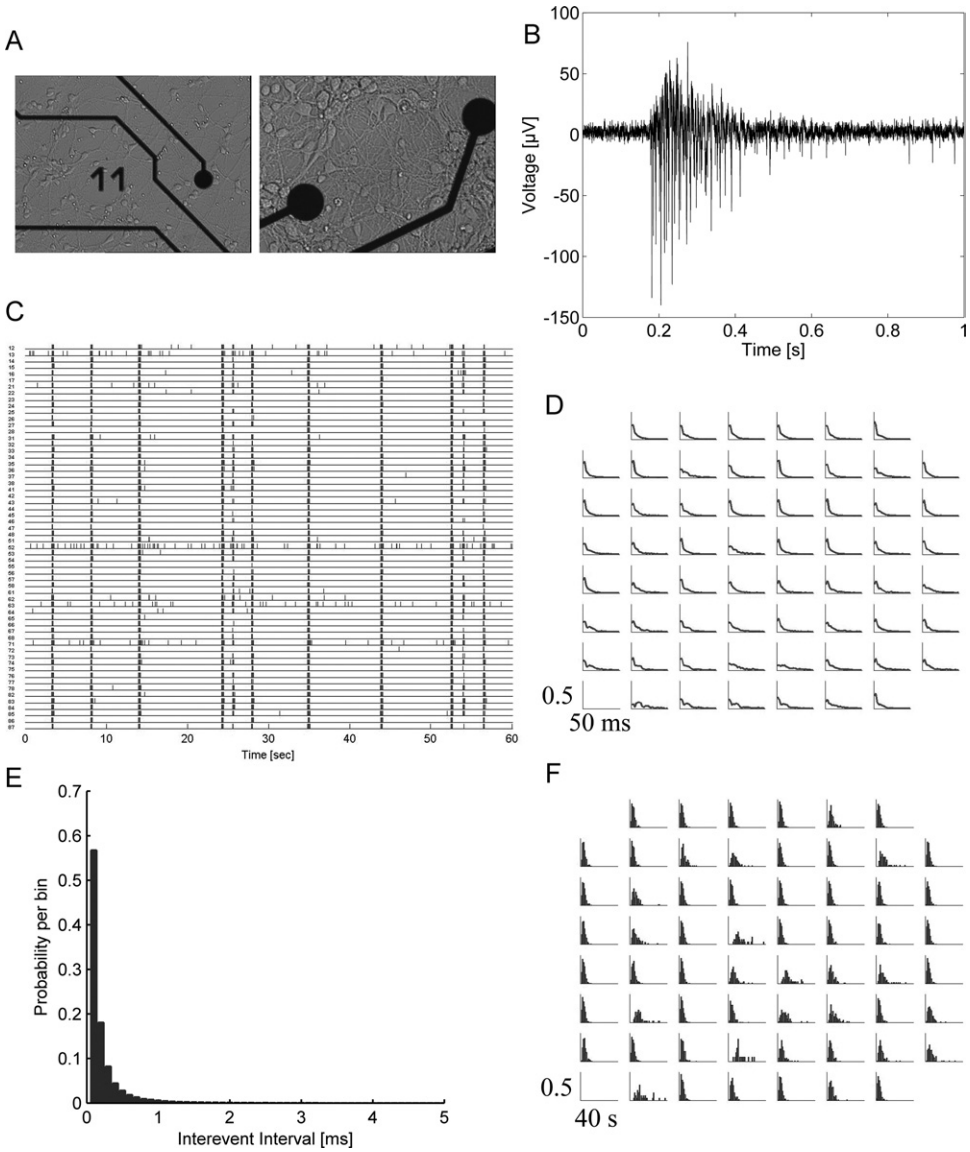

Fig. 1. Electrophysiological activity of cultured neurons is composed of synchronized bursts, mixed with random spikes. (A) Dissociated cortical neurons coupled to a MEA and randomly developing their neurites and synaptic connections 5 days after seeding. (B) Electrophysiological activity recorded from one microelectrode. (C) Raster plot of activity: each row corresponds to a recording site and each small vertical line to a detected spike. (D) ISI distributions depicted over an eight by eight grid, reproducing the MEA layout. (E) An example of IEI distribution: most values are concentrated below 1 ms. (F) IBI distributions (eight by eight grid, MEA layout). Data from one culture, 27 DIV, 1 h recording.

Cross-correlograms

To characterize the level of synchronization among multi-unit recordings, the correlation analysis was applied to spike trains and to burst event trains (Chiappalone et al., 2007).

Cross-correlograms were built according to the method of the activity pairs described by (Eytan et al., 2004): given two trains (i.e. *X* and *Y*), recorded from two electrodes of the MEA, we counted the number of events in the *Y* train within a time frame around the *X* event of ±T (T usually set at 150 ms), using bins of amplitude $\Delta\tau$ (usually set at 1 ms). The cross-correlation function $C_{xy}(\tau)$ was obtained by a normalization procedure, according to the following formula,

$$C_{xy}(T)=\frac{1}{\sqrt{N_x N_y}}\sum_{t_i=\left(T-\frac{\Delta T}{2}\right)}^{\left(T+\frac{\Delta T}{2}\right)} X(t_s)\,Y(t_s-t_i) \qquad (1)$$

where t_s indicates the timing of an event in the *X* train, N_x and N_y are the total number of events in the *X* and in the *Y* train respectively, $\Delta\tau$ is the bin size. Equation (1) yields the symmetry between $C_{xy}(\tau)$ and $C_{yx}(\tau)$ (i.e. $C_{xy}(\tau)=C_{yx}(-\tau)$) (Eytan et al., 2004).

In particular, the cross-correlogram coefficient, $C_{xy}(0)$

$$C_{xy}(0)=\sum_{T=-k\cdot\frac{\Delta T}{2}}^{k\cdot\frac{\Delta T}{2}} C_{xy}(T) \qquad (2)$$

represents the area of the cross-correlogram around the zero bin (k is the number of bins) and it is evaluated in order to quantify the synchronization level among the recording channels. From Equation (2), we also calculated the coincidence index (CI_0) (Jimbo et al., 1999; Tateno and Jimbo, 1999) as the ratio of the integral of a cross-correlation function in a specified area around zero (i.e. $C_{xy}(0)$) to the integral of the total area, according to:

$$CI_0 = \frac{\sum_{r=k\frac{\Delta T}{2}}^{k\frac{\Delta T}{2}} C_{xy}(T)}{\sum_{T=-T}^{+T} C_{xy}(T)} = \frac{C_{xy}(0)}{\sum_{T=-T}^{+T} C_{xy}(T)} \quad (3)$$

Neuronal avalanche detection

Starting from the work of Beggs and Plenz (2003, 2004), a neuronal avalanche can be defined as an event of widespread spontaneous electrical activity over the MEA, preceded and followed by a silent period.

Recordings can be divided into time windows of duration Δt (called *bins*); inside each bin the spatial distribution of activity over the MEA represents a *frame*. A frame which does not contain any spike is called a *blank frame*. An electrode is *active* in a time bin Δt if it records at least one spike inside that time window. Thus, a frame is active if it recruits at least one active electrode. Following these definitions, a *neuronal avalanche* is a continuous sequence of active frames, preceded and followed by at least one blank frame.

In dissociated cortical cultures, we can detect both very short avalanches, composed of a single spike on a single electrode, and avalanches that include thousands of spikes and all the recording electrodes. Consequently, the *avalanche size* can be defined either as the total number of active electrodes within an avalanche, taking into account multiple activations of the same electrodes (definition 1), or as the number of electrodes being active at least once inside an avalanche (definition 2). The duration of an avalanche is usually called *avalanche lifetime* and is expressed in number of bins Δt. The two definitions of avalanche size are equivalent only if all the electrodes are active at most once inside an avalanche. This condition is not always verified in dissociated cultures, because of high-frequency firing activity within bursts.

From the spike-detected signals, we computed neuronal avalanches and we derived the relative histogram of avalanche sizes (following both definitions) and lifetimes: in practice, we counted, from the data set, the number of avalanches falling into each bin of the histogram and then we normalized the histogram to the total number of detected avalanches. Therefore, the height of each histogram bar represents the proportion of avalanches of a given size or lifetime.

These histograms are generally represented in bilogarithmic scale in order to show whether the distribution follows a power law: thus, if the probability of observing an avalanche of size s is expressed by $P(s)=as^b$, that appears as a linear relationship in the bilogarithmic scale with slope b.

The electrophysiological recordings were analyzed for the detection of neuronal avalanches at bin widths of 0.2-0.4-0.6-0.8-1-2-4-8-16 ms.

All the algorithms for the off-line signal processing were developed using Matlab 7.0, Release 14 (Mathworks Inc., Natick, MA, USA).

Power-law regression of the distribution curves of avalanche sizes and lifetimes

In order to assess if the distributions of avalanche sizes and lifetimes follow a power law, we performed a parametric non-linear fitting of the data, using a power law model $P(x)=ax^b$, where x is the independent variable (e.g. avalanche sizes' or avalanche lifetimes' occurrence frequencies) and a, b are fitting parameters. We excluded from the fitting the first bin, corresponding to avalanches of unit-dimension (and unit-duration), and the last bins of the histogram, corresponding to avalanches whose probability is less than 1% of the maximum value of the distribution. Finally, to evaluate the efficiency of the fitting we considered the *root mean squared error* (RMSE) or *standard error* of the regression.

Interevent (IEI), interspike (ISI) and interburst interval (IBI) histograms

The result of the spike detection is a collection of point processes, one for each recording channel, where each detected spike is represented as an impulse. The probability density of time intervals between adjacent spikes is called the ISI distribution, and it is a useful statistic for characterizing spiking patterns (Dayan and Abbott, 2001) (Fig. 1D).

Considering the electrophysiological activity of the whole culture, we derived the probability density of time intervals between successive spikes occurring at all the electrodes, namely the IEI distribution (Beggs and Plenz, 2003). Computing the average value of the IEI distribution, we obtained for every considered culture an estimation of the average time between two successive activations of any pair of electrodes in the array (Fig. 1E). Similarly, the average value of the ISI distribution is an estimate of the average time between two successive spikes on the same elec-

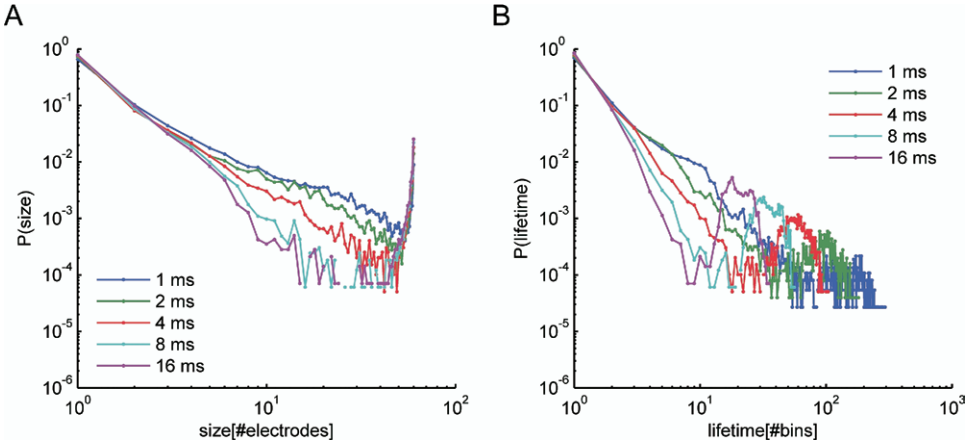

Fig. 2. Avalanche size and lifetime distributions appear supercritical when using time bins ≥1 ms. As the bin width increases, medium-size avalanches merge, increasing the probability of detecting avalanches that encompass the whole network. (A) Avalanche size distribution computed as the number of active microelectrodes involved in each avalanche. (B) Avalanche lifetime distribution computed as the number of time bins (bin width=0.2 ms). Data obtained from a single culture, 27 DIV, 1 h-recording.

trode. The average IEI (or ISI) was obtained by calculating the average value of the IEI (or ISI) distribution over the time interval $[0, T_{max}]$; T_{max} was determined as the average time interval $[-T_{max}, T_{max}]$ corresponding to the 99% of the area of the mean cross-correlogram (averaging cross-correlograms between all possible pairs of electrodes). T_{max} ranged from 50 to 80 ms, so we considered T_{max}=65 ms for all cultures.

Finally, the probability density of time intervals between two successive bursts on a single electrode is the IBI distribution (Fig. 1F).

Shuffling methods

In order to validate the statistical significance of our results, we compared them with the ones obtained by applying the avalanche detection algorithm to a shuffled version of the recorded data. We applied two different shuffling methods, namely single electrode shuffling (SE) and all electrodes shuffling (AE), to one long-lasting experiment.

More specifically, the SE shuffling method firstly binned each electrode's recording by means of an appropriately wide temporal

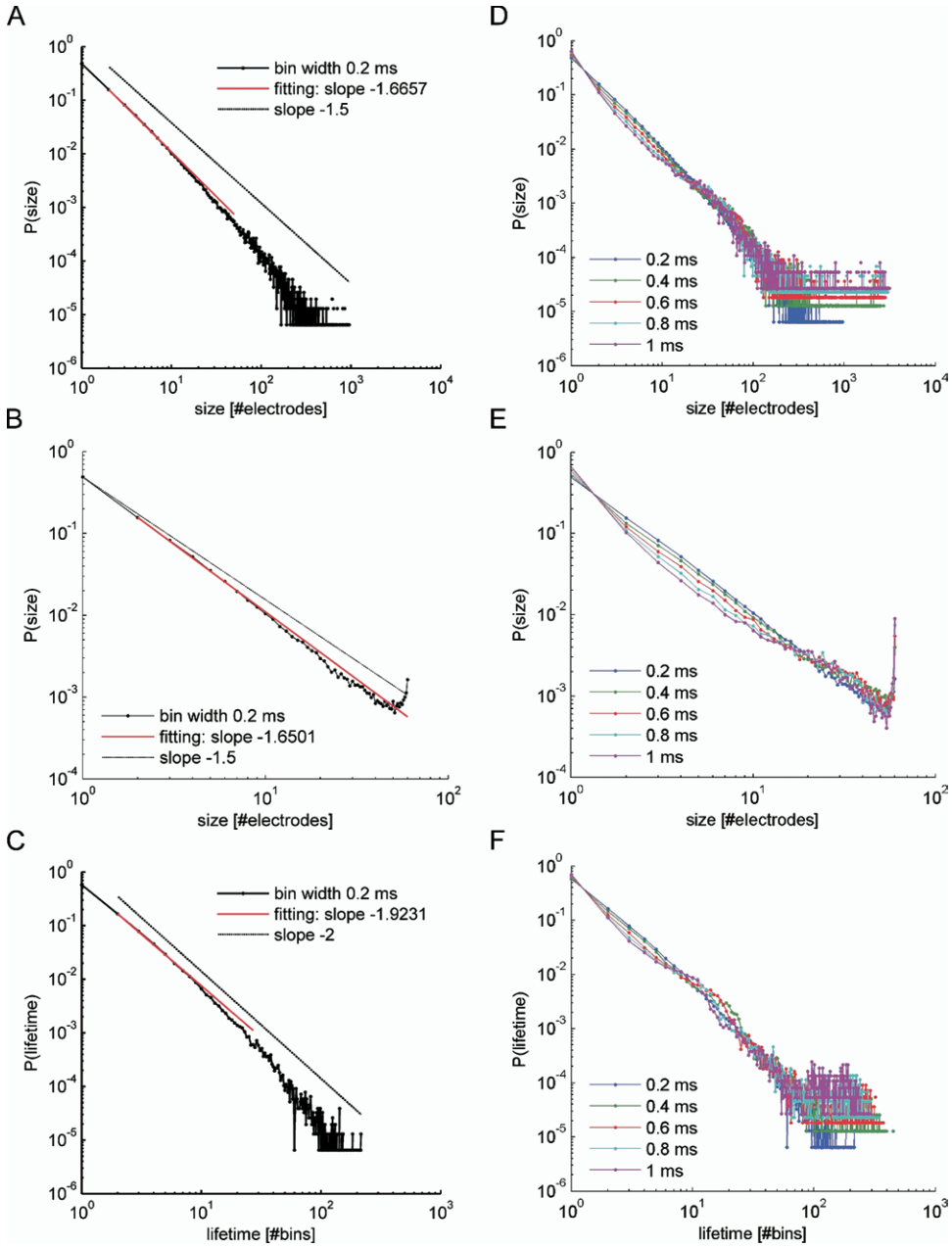

Fig. 3. Size and lifetime of neuronal avalanches follow a linear relationship in bilogarithmic plots, indicating a power law distribution. (A) Avalanche size distribution, computed according to definition 1. (B) Avalanche size distribution, computed according to definition 2 (cf. Experimental Procedures). (C) Avalanche lifetime distribution, measured in number of bins. Every curve is compared with the critical power law distribution (exponent −1.5 for size and −2 for lifetime) and the corresponding power law fitting (slope of fitting reported in the legend). Bin width=0.2 ms. (D–F) Same distributions as in (A–C) but the results are obtained with different bin widths (0.2-0.4-0.6-0.8-1 ms). Data obtained from one culture, 27 DIV, 1 h-recording.

bin, and then uniformly permuted the order of the bins. This resulted in reshaping the spike train recorded by each electrode while preserving its mean firing rate (relative position of each spike inside a bin was preserved). In this way, we disrupted possible spatial relationships within the activities recorded by different electrodes. The AE shuffling method performed the same manipulation explained for the SE shuffling method to all electrodes' recordings at a time. This means that the same temporal permutation was applied to all the electrodes (preserving, under certain circumstances, possible spatial relationships). We applied both methods by using two different bin widths: 2 ms (the one used for the spike detection) and 0.2 ms (used for the avalanche detection).

Rescaling of arrays

Each electrode array is a square eight by eight grid without the corners, thus having 60 electrodes. The interelectrode distance (IED) between each electrode and its nearest neighbor is 200 μm. To examine how the spatial scale given by the IED influences the power law distributions, we performed the same rescaling of arrays described in Beggs and Plenz (2003). Briefly, rescaling was accomplished by removing some of the intercalated electrodes from the analysis, while still maintaining a square array. This also reduced the number of electrodes considered in the analysis. To create an IED of 400 μm, a regular array of four by four electrodes was chosen from the eight by eight array, which resulted in twice the distance between the electrodes from the original array. This rescaled array could be fit onto the original array in four ways, although each way caused one of the corner electrodes to be missing, leaving only 15 electrodes (cf. Fig. 4B, inset). The data for this rescaled array were obtained from 15 electrodes for each of the four ways and averaged. A similar rescaling was done to create an IED of 600 μm, leaving only eight electrodes (a three by three array with one corner missing). We hypothesized a simple linear correspondence between the IED and the corresponding average IEI, as reported in the literature (Beggs and Plenz, 2003), and this relation was also confirmed by our data; thus we binned spike trains at 0.4–0.6 ms for the 400–600 μm IED, respectively.

Neuronal network model

A computational model was developed to provide a comparison with the avalanche behavior found in the experimental results, to help in the interpretation of the data with respect to the main statistical features of the network (i.e. spiking and bursting dynamics) and to give some insights of the network topology. We implemented a large-scale neuronal network model showing sub-, super-, and critical states by mimicking the electrophysiological activity of cultured cortical neurons under spontaneous condition and chemical manipulation. Several models have been developed to describe and explain the critical behavior of the brain (Chialvo, 2004, 2006) and of neuronal networks *in vitro* (Abbott and Rohrkemper, 2007). However, the proposed models are quite abstract and discard the dynamics of single neurons: Corral et al. (1995) implemented a lattice model of integrated and fire oscillators inspired by the dynamics of earthquakes; Park et al. (2005) developed a model inspired by graph theory; more recently, Abbott and Rohrkemper (2007) adapted a simple model of neuronal growth (van Ooyen and van Pelt, 1996) to demonstrate the presence of avalanches in cultured slices (Abbott and Rohrkemper, 2007).

Following the approach proposed by Izhikevich (2003), we developed a neuronal network model made of 1000 spatially distributed and synaptically connected neurons. We considered two different types of neurons to model excitatory and inhibitory populations of neurons, respectively: the former belongs to the family of regular spiking neurons while the latter to the family of fast spiking neurons (Izhikevich, 2004). Regular spiking neurons fire with a few spikes and short ISI at the onset of a stimulation. Differently, fast spiking neurons exhibit periodic trains of action potentials at higher frequencies without adaptation. To preserve some characteristics of the structure of *in vitro* cortical neurons, we set the ratio between excitatory and inhibitory neurons to 4:1 (Braitenberg and Schultz, 1991; Marom and Shahaf, 2002). These two families of neurons were connected in a scale-free topology by following the hypothesis proposed by Chialvo (Chialvo, 2004; Eguiluz et al., 2005) to obtain a large-scale neuronal network showing a critical behavior. The scale-free topology was implemented by following the model devised by Barabasi and Albert (1999). More specifically, we firstly defined the network size (i.e. the number of neurons), the number of links that a new node can establish with the existing ones and the initial connectivity matrix (with a size$\ll$of the desired size). Secondly, by means of the specific preferential attachment procedure described in the aforementioned model (Barabasi and Albert, 1999), we changed the

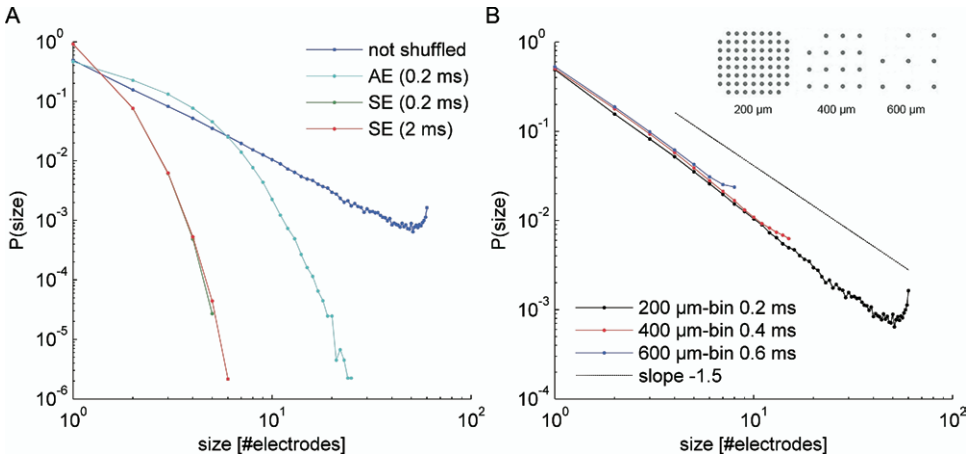

Fig. 4. Shuffling procedures and rescaling of arrays. (A) Avalanche size distribution for a selected experiment (one culture, 27 DIV, 1 h-recording) compared with shuffled data by means of three different shuffling methods, namely AE-0.2 m, SE-0.2 ms and SE-2 ms (cf. Experimental Procedures). By applying the avalanche analysis to the shuffled data, the linear distribution is partly (AE-0.2 ms) or completely (SE, both time bins) lost. (B) Avalanche size distribution for the same aforementioned experiment compared with data from rescaling of arrays to obtain IED=400 μm (red line) and IED=600 μm (blue line); the bin size is varied to account for the linear relationship between IED and average IEI. The rescaling procedure demonstrates that the avalanche size distribution does not change its slope if we vary the bin size according to the corresponding average IEI. Inset, sketch of the rescaled MEAs and corresponding IED.

connectivity of the network by establishing connections to previously unlinked nodes. In this way, the network model presents a few highly connected hubs and several less connected nodes (Fig. 11D).

We considered the choice of scale-free architecture to be appropriate in light of previous experimental results obtained by Eytan and Marom (2006) for the same experimental preparation. Actually, they demonstrated that the distribution of firing rates during the early phase of a network burst is broad and described by a power law, which is consistent with a scale-free topology of connectivity.

Spontaneous activity was obtained by introducing a randomly distributed stimulation mimicking the effect of fluctuations in the membrane potential (Buchmann and Schulten, 1987) due to the background activity. Furthermore, the effect of chemical manipulations (i.e. application of BIC and ACh) on the network behavior was taken into account. As reported in the literature, the effect of ACh in cortical neurons is to enhance the persistent spiking activity of individual neurons (Klink and Alonso, 1997; Fransen et al., 2006; Hasselmo, 2006) by means of a strong depolarization of the resting membrane potential (Haj-Dahmane and Andrade, 1996). To achieve this behavior, we emulated the perfusion of ACh in the network model by reducing the spiking threshold of the neurons in order to enhance the firing probability.

The effect of BIC, a strong antagonist of the inhibitory synaptic receptors $GABA_A$ (Chebib and Johnston, 1999), was simply mimicked by multiplying each inhibitory connection by the factor $(1-BIC)$, with $0 \leq BIC \leq 1$.

All the simulations lasted 60 s with an integration time step of 0.1 ms. The simulation output was then peak-detected by means of a simple hard-threshold algorithm. To compare the simulated results with the experimental data 60 of 1000 neurons (retaining the ratio between excitatory and inhibitory neurons and a scale-free topology) were picked up and considered in the avalanche analysis. Two main assumptions were made for this model: firstly, the 1:1 correspondence between neurons and microelectrodes. Although this is not biologically realistic, the effectiveness of this simplification was previously demonstrated by the authors (Massobrio et al., 2007). Secondly, the choice of a pool of neurons is not influenced by spatial constraints: in fact the neurons are modeled as punctual processes and no axonal conduction delay is taken into account.

RESULTS

Neuronal avalanche detection depends upon the time scale of observation

Beggs and Plenz (2003, 2004) proposed innovative results about propagation of spontaneous electrical activity (measured as local field potential, LFP) in rat cortical slices, cultured over MEAs. Highly synchronized episodes of activity, preceded and followed by silent periods and generally appearing at all electrodes, actually hide complex spatio-temporal patterns in which activity develops over a distributed area in an avalanche-like form. The term "avalanche" is not used at random: looking at the distribution of size and duration of these events, they found that it follows a power law, as other self-organizing natural phenomena, included real avalanches (Bak et al., 1987, 1988; Bak, 1996). Moreover, the power law exponent value (-1.5) found for the avalanche size distribution suggested that the widespread electrophysiological activity within these neuronal avalanches underlies a critical process (Zapperi et al., 1995). Nevertheless, in order to detect avalanches from the activity of cortical slices, it was crucial to reduce the time scale of observation, binning the LFP data according to a bin width of 4 ms (Beggs and Plenz, 2003). In addition, time interval distributions of successive LFPs on individual electrodes revealed that they were at least 24 ms apart from each other (Beggs and Plenz, 2003): therefore, the time window used to detect avalanches from LFP data is approximately one order of magnitude smaller than the refractory period on a single channel.

Starting from this consideration, we derived from the spiking activity of dissociated cortical cultures the ISI distribution on individual electrodes and the IEI distribution on the whole MEA (cf. Fig. 1). The IEI distribution showed the same trend for every considered network and average values usually lie below 1 ms (0.34 ± 0.11 ms, mean$\pm$S.D., four cultures, 4th week *in vitro*). Also ISI distributions exhibited a fast decay toward zero, although, due to the physiological limit of refractoriness, average values were approximately one order of magnitude higher than intervals between successive events on different electrodes (7.35 ± 1.12 ms, mean$\pm$S.D., four cultures, 4th week *in vitro*). The ratio between the IED (i.e. 200 μm) and the average IEI (i.e. 0.3 ms) in cultures of dissociated neurons was about 10 times higher than in cortical slices ($\sim$500 mm/s and $\sim$50 mm/s respectively), mainly because we considered spikes instead of LFPs (Freeman, 1975; Hsu et al., 2007).

This ratio can be also regarded as a rough estimate of the maximum propagation velocity of electrophysiological activity in cultured networks. In a recent study (Jacobi and Moses, 2007), in which the neural activity of one-dimensional rat hippocampal cultures patterned in lines over MEAs was investigated, the reported propagation velocity ranged from 30 to 300 mm/s within each culture. In addition, a study conducted on planar cultures of dissociated hippocampal neurons (Bonifazi et al., 2005; Ruaro et al., 2005) reported an estimate of the maximum propagation speed of 350 mm/s. All these values are in agreement with our estimate of average IEI.

Considering the ISI and IEI ranges in our cultures, we expected to find a bimodal distribution of avalanche sizes and lifetimes, characteristic of a supercritical state (Bak, 1996; Chialvo, 2006) by using bin widths of 2–4 ms: at this time scale, every network burst that spreads over the MEA can be seen as a single avalanche that involves the whole dynamical system. Therefore, the network appears as a system showing a supercritical behavior, with an all-or-none activity (Fig. 2).

Starting from these initial results, we reduced the time scale of observation in order to account for IEI values and the use of a bin width of 0.2 ms enabled us to reveal several avalanches of different size and duration within each burst.

Avalanche size and lifetime distributions obtained from a typical culture are shown in Fig. 3: these results illustrate the dynamic behavior found in our dissociated cortical cultures. At a fine timescale (0.2 ms), both neuronal avalanche sizes and lifetimes follow a power law distribution, very close to the behavior Beggs and Plenz (2003) report as critical (i.e. with exponents close to -1.5 for sizes and

−2 for lifetimes). As the window increases from 0.2–1 ms, curves shift from a linear relationship to a bimodal distribution, typical of a supercritical state (Bak, 1996). Therefore, the time scale used for detecting avalanches ($\sim 10^{-1}$ ms or ~1 ms) has to be adjusted in function of the signals' time scale to determine whether the developing network displays a power law distribution and reaches a critical state.

To verify that what we observed by using a small bin width (i.e. 0.2 ms) is not a mere artifact of the method, we applied two different shuffling algorithms to our data and then we analyzed them again for the avalanche distributions (cf. Experimental Procedures).

As we expected, the application of the avalanche algorithm to the data shuffled by means of the AE shuffling method did not result in significant differences when we used the 2 ms-wide bin. This behavior can be explained by considering that the most significant results were related to shorter bin widths (<1 ms). Thus, the shuffling algorithm applied by using a wider time bin (2 ms) is likely to move the fine temporal structures giving rise to interesting avalanche dynamics all together. As expected, the same method applied by using a time bin of 0.2 ms only caused a partial disruption of the activity patterns. In fact, on the one hand the finer time resolution allowed changing of the temporal spike train structure on a subtler level. On the other hand, given that the AE shuffling method entailed the same temporal permutation for all the electrodes (cf. Experimental Procedures), some of the spatial structure of the electrophysiological activity was preserved, thus preventing a complete loss of the power law dynamics. Instead, the latter was achieved through the application of the SE shuffling method with both a 2 ms and 0.2 ms-wide bin (getting closer to the behavior one would expect for Poissonian spike trains). This result was expected as well, and demonstrates the intrinsic fine spatio-temporal structures found in dissociated cultures (Fig. 4A).

Additionally, to verify that the avalanche distribution obtained by binning data at 0.2 ms is not affected by the sampling rate value (usually 10 kHz), we performed one recording by varying the sampling frequency (10 kHz and 25 kHz) and we found qualitatively the same results (data not shown).

Finally, we applied the same rescaling procedure of the arrays described in Beggs and Plenz (2003) to examine how the IED affects the power law distribution of avalanches (cf. Fig. 4B). The average IEI linearly scales with the IED (data not shown), thus the bin width used for the analysis has to be varied according to the IED. For the same experiment shown in Fig. 3, we binned the data at 0.4–0.6 ms for IED=400–600 μm, respectively, and we obtained the same power law occurring for the complete dataset. This result suggests that the power law is independent of the IED and that the network behavior is scale-free.

Because of these experimental evidences, we decided to focus on bin widths ≤1 ms and, in particular, we compared results obtained from different cultures at 0.2 ms, correlating different avalanche distributions with other parameters describing the network dynamics. The power law regression of the distributions obtained by using the two different definitions of avalanche size (cf. Experimental Procedures) provides equivalent exponent values: therefore, in the following paragraphs, we considered only the avalanche size as number of electrodes involved in an avalanche (i.e. definition 2).

Neuronal cultures developing *in vitro* self-organize at a mature developmental stage displaying different dynamic states

Six cultures were monitored during development from the 1st to the 6th week *in vitro* and their spontaneous electrical activity was recorded. To evaluate the capability of dissociated neurons to self-organize in a critical state, we focused on recordings between 21 and 42 DIV, i.e. in the mature developmental stage (van Pelt et al., 2005; Chiappalone et al., 2006b).

Fig. 5A shows the number of bursting channels for each culture (mean±SEM, calculated in the key period of development, i.e. from the 4th to the 6th week *in vitro*). Moreover, we reported also the mean bursting rate (MBR), averaged from the 4th to the 6th week *in vitro* (Fig. 5B), to provide an overview of the different levels of activity recorded from different cultures.

Fig. 5C shows the number of avalanches detected per minute as a function of DIV: the average number of avalanches is low until the 3rd week *in vitro*; then, it increases and lies between 1500 and 3000 avalanches/min during the whole mature phase. Nevertheless, there is variability among cultures, showing that every network develops in a different way according to some factors, such as the actual plating density, the cellular composition, the relative amount of glia cells and the coupling with the electrodes. Looking for these factors is beyond the aim of this work; however we wanted to show how the avalanche distribution changes during development and in different cultures.

Once a culture had reached the mature stage, it showed a preferred behavior (critical or quasi-critical, subcritical or supercritical), even if some deviations are possible. Thus, not all cultures evolve toward criticality during development: for example, two cultures (#1 and #4) display a critical behavior between the 4th and the 5th week *in vitro*; one culture (#3) exhibits a subcritical behavior, while three cultures (#2, #5 and #6) generate a strong supercritical behavior that persists during the majority of the mature stage. Though the observed cultures did not share a common pathway of development, they nonetheless demonstrate that networks of dissociated neurons can approach a critical state in the mature phase, giving rise to events that corresponds to the description of neuronal avalanches.

For further analysis, we considered all cultures (i.e. both acute long-lasting experiments and developmental recordings) in the 4th week *in vitro*. Averaging the results of four experiments on different cultures, which displayed a critical behavior in the mature age, we obtained an average slope of −1.60±0.09 (mean±S.D., RMSE$<10^{-3}$) for the avalanche size and −1.86±0.13 (RMSE$<10^{-2}$) for the

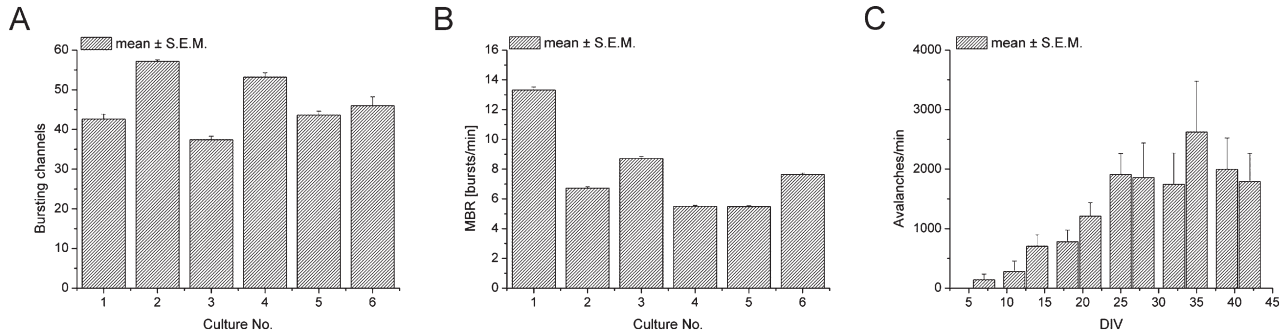

Fig. 5. Neuronal avalanche dynamics varies in different cultures and during development. (A) Number of bursting channels (mean±SEM, averaging recordings from 21 to 42 DIV) for each of the six cultures monitored during development. (B) MBR of each culture (mean±SEM) in the mature developmental stage (21–42 DIV): different networks show different levels of activity, with burst rate varying from 5 to 14 bursts/min. (C) The number of avalanches recorded per minute in function of DIV (mean±SEM, averaging data from six cultures) is extremely variable among cultures, though they display a similar behavior: it is lower during the first 3 weeks *in vitro*, then it increases as the network reaches the mature phase.

avalanche lifetime. Similarly, averaging the results of two subcritical cultures, we obtained a slope of -2.03 ± 0.12 (RMSE$<10^{-3}$) for the size and -2.45 ± 0.20 for the lifetime (RMSE$<10^{-3}$). Lastly, averaging the results of three supercritical cultures, we obtained -1.88 ± 0.17 (RMSE$<10^{-2}$) and -2.19 ± 0.16 (RMSE$<10^{-2}$), respectively for the size and the lifetime.

To investigate which statistics correlate with the network dynamic behavior, we studied different parameters describing neuronal activity, namely mean firing rate, MBR, IBI distribution, burst duration, mean spiking frequency within bursts, percentage of random spikes and cross-correlograms computed on burst event trains. All these quantities contribute to the definition of the dynamic state of the culture, but we focused on the percentage of random spikes (i.e. the fraction of spikes outside bursts) and the CI_0 between all pairs of electrodes, because only these parameters exhibited a clear relation with the avalanche distribution. The former is a measure of the proportion between spikes included within bursts and random spikes outside bursts (so it is a simple way to quantify the level of burstiness of the network); the latter measures the synchronization of bursts among all electrodes.

Neuronal avalanche distribution is correlated with the degree of synchronization of bursts and the proportion between spiking and bursting activity

Fig. 6 shows the results of the avalanche analysis applied to three representative experiments (cultures #3, #4 and #6 during the 4th week *in vitro*), selected to exemplify the different dynamic states found in mature dissociated cultures: these curves show a progression from a markedly subcritical distribution (#3) to a strongly supercritical one (#6), through a distribution (#4) that approaches the critical state for both avalanche sizes and lifetimes.

These results correlate with the corresponding distributions of the percentage of random spiking activity and the CI_0: in Fig. 7 we reported a box-plot representation of the two histograms obtained by considering all cultures (four critical, two subcritical and three supercritical). These statistical distributions are different as confirmed by suitable statistical tests (we applied the Kruskal-Wallis nonparametric test, instead of a t-test, because the normality assumption was not verified by our datasets (Kolmogorov-Smirnov normality test)) (ANOVA for ranks, Kruskal-Wallis test: CI_0, H (N=3356)=1071.106, $P\leq0.001$; percentage

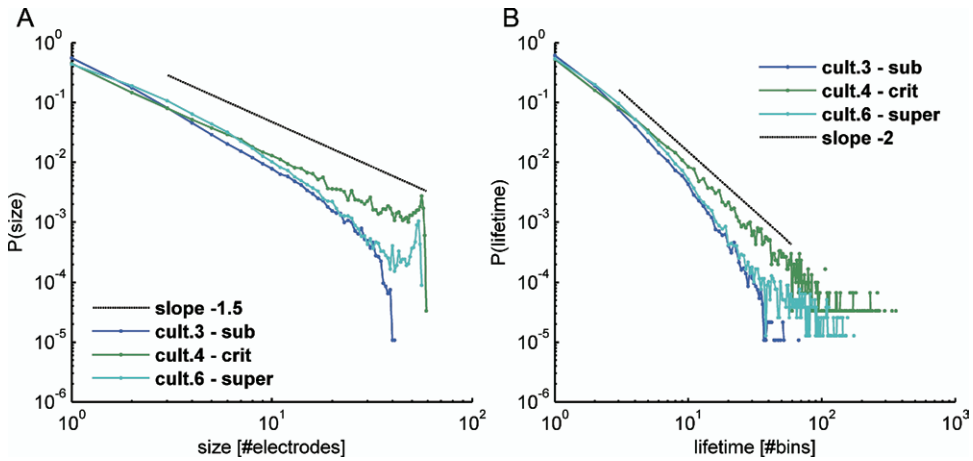

Fig. 6. In mature cultures we can observe different dynamic behaviors, exemplified by three selected cultures. (A) Avalanche size distributions. (B) Avalanche lifetime distributions. Both histograms are compared with power laws whose exponents are -1.5 and -2, for the size and for the lifetime, respectively.

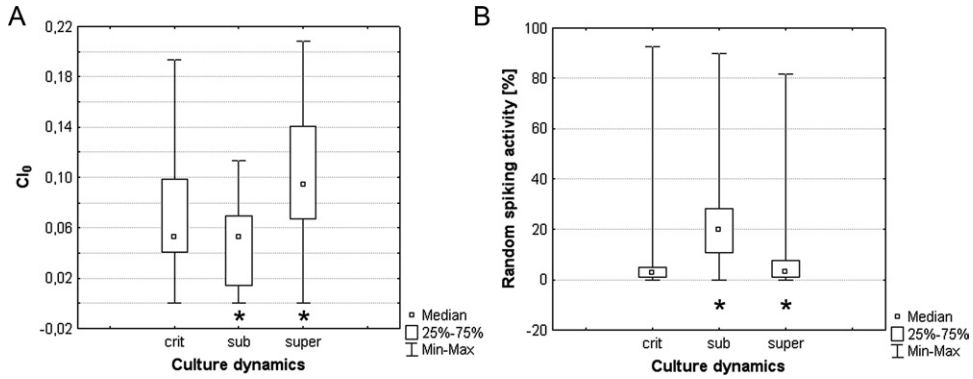

Fig. 7. Different avalanche distributions correspond to different global activities, both in the synchronization level and the proportion between random spikes and bursts. (A) Box plots of CI_0 distributions for critical, subcritical and supercritical cultures. (B) Box plots of percentage of random spiking activity distributions for the same groups of cultures. Data obtained from four critical, two subcritical and three supercritical cultures in the 4th week of development. Stars indicate statistically significant differences with respect to the critical condition.

of random spiking activity, H (N=3264)=1112.986, $P \leq 0.001$).

Critical distributions of avalanche sizes and lifetimes correlate with average synchronization of bursts among electrodes, while subcritical and supercritical distributions correspond to low-level synchronization and to high-level synchronization, respectively. In addition, we noticed that, in cultures tending to criticality, most spikes are concentrated within bursts (i.e. median and 25%–75% percentile values of the proportion of random spikes are lower), whereas the other cultures have, on average, a less compact bursting activity (the trend is more evident for subcritical networks as shown in Fig. 7B).

Specific chemical manipulations confirm the correlation between avalanche dynamics, synchronization and random spiking activity

To validate these results, we also analyzed how the distribution of avalanches changes in response to specific chemical treatments that affect synchronization and bursting dynamics.

Under application of 10 μM ACh, the bursting activity markedly increases and desynchronizes (Chiappalone et al., 2007). On the contrary, with 30 μM BIC the synchronization within bursts and the percentage of random spikes increases (Chiappalone et al., 2007).

In Fig. 8 we compared the box-plots of the CI_0 and the percentage of random spiking distributions under control condition and chemical stimulation. Both in ACh and BIC, CI_0 distributions are significantly different from the control condition, as confirmed by suitable statistical tests (we applied the Mann-Whitney U nonparametric test, instead of a t-test, because the normality assumption was not verified by our datasets (Kolmogorov-Smirnov normality test)) (Mann-Whitney (U) test: ACh vs. control condition, Z=7.803, $P \leq 0.001$; BIC vs. control condition, Z=−11.462, $P \leq 0.001$) (cf. Fig. 8A–B); also the percentage of random spiking activity varies significantly (Mann-Whitney (U) test: ACh vs. control condition, Z=−9.618, $P \leq 0.001$; BIC vs. control condition, Z=−12.0363, $P \leq 0.001$) (cf. Fig. 8C–D).

The effects of ACh and BIC on neuronal avalanche features are shown in Fig. 9A and Fig. 9B respectively, pointing out avalanche size distributions in the control condition and under chemical treatment for two representative experiments.

In the case of application of Ach, starting from a near-critical dynamics, we obtained a subcritical distribution, with a slope far from −1.5 (−3.620±1.096, mean±S.D., three cultures). Contrarily, the application of BIC led to a supercritical behavior, with a fitting slope greater than −1.5 in the initial half and a more pronounced peak in the tail (−2.199±0.141, mean±S.D., three cultures).

Consequently, the link between avalanche dynamics, synchronization and random spiking proportion was confirmed by chemical stimulation results: when synchronization was completely lost and random spiking activity strongly enhanced (i.e. adding ACh), the network exhibited subcriticality, whereas when synchronization within bursts was markedly increased (i.e. adding BIC), network dynamics switched to a supercritical state.

Scale-free large-scale network models compare favorably with experimental data

To confirm some of the hypotheses made for the analysis of the experimental data and to better understand the obtained experimental results, we simulated the spontaneous activity of the scale-free neuronal network model previously described (cf. Experimental Procedures). The power law distribution of connectivity degree among the 1000 network nodes is shown in Fig. 11D. Starting from this global connectivity, 60 neurons were selected by maintaining the scale-free topology of connections and the physiological ratio between excitatory and inhibitory populations of neurons (i.e. 4:1).

Firstly, the proposed computational model reproduced the same IEI distribution (IEI_{avg}=0.35 ms) obtained from experimental data, thus suggesting that the time scale of the simulated activity closely resemble the experimental one (Fig. 10A).

Secondly, the distribution of avalanche sizes and lifetimes depended upon the time bin used for the analysis, as

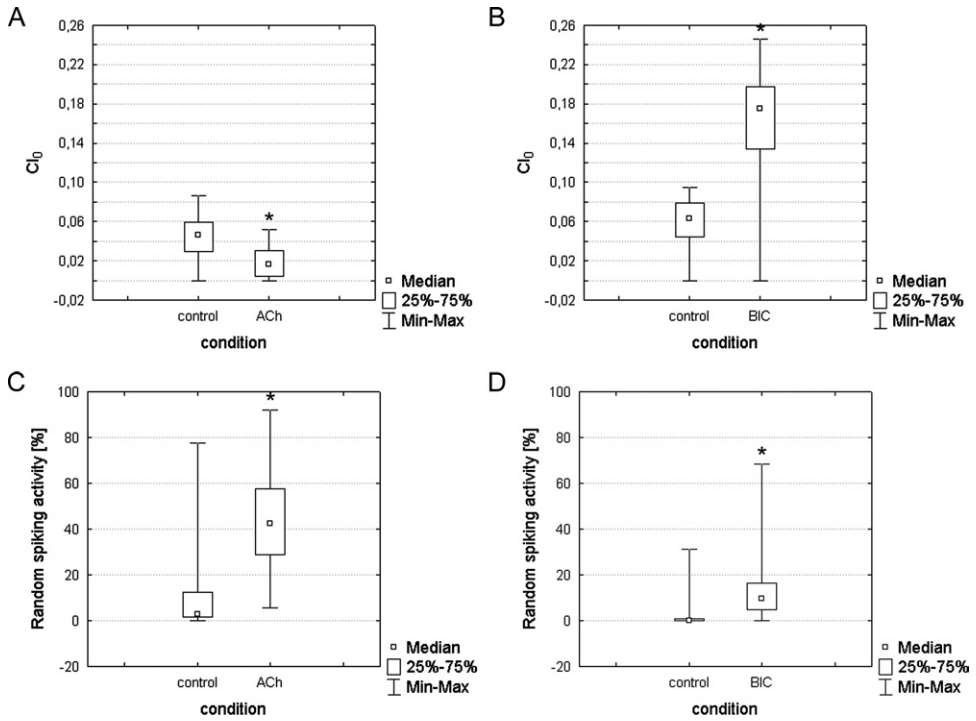

Fig. 8. Comparing the bursting behavior between the control condition and under drug treatment, we confirmed the link between neuronal avalanche dynamics, synchronization and proportion of random spiking activity. (A, B) Box plots of CI_0 distributions under ACh 10 μM application (A) and BIC 30 μM application (B). (C, D) Box plots of percentage of random spikes distributions for ACh 10 μM (C) and BIC 30 μM (D). Data obtained from six cultures (three treated with ACh and three with BIC). Stars indicate statistically significant differences with respect to the control condition.

well as for the experimental data (Fig. 10B–C): therefore, the network model also presented an avalanche behavior similar to that found in the electrophysiological activity of cultures of dissociated neurons, when considering the spiking activity.

In addition, we simulated the behavior of the same network under chemical treatments (i.e. ACh and BIC). These simulated data were processed at a bin size of 0.2 ms, as well as for the experimental data previously reported.

By modeling the spontaneous condition, neuronal avalanche size and lifetime distributions approach critical power laws at a 0.2 ms bin width (Fig. 11A–C, black line). As already stated, these results are in good agreement with those obtained from the experimental data (cf. Fig. 3). By increasing the bin size (i.e. bin widths ~1 ms), the avalanche features' distributions switch from a critical to a supercritical behavior, thus further validating the choice of the bin size (cf. Fig. 10B–C).

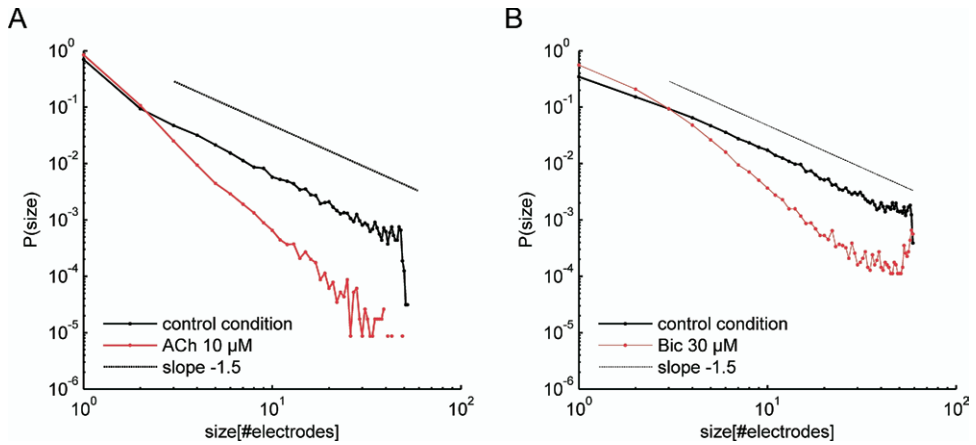

Fig. 9. The proportion between bursting and random spiking activity, as well as the synchronization among bursts, determines changes in the neuronal avalanche distribution. (A) Avalanche size distributions found in the control condition and by adding ACh 10 μM. (B) Avalanche size distributions found in the control condition and by adding BIC 30 μM. Both curves are compared with -1.5 and -2 power laws.

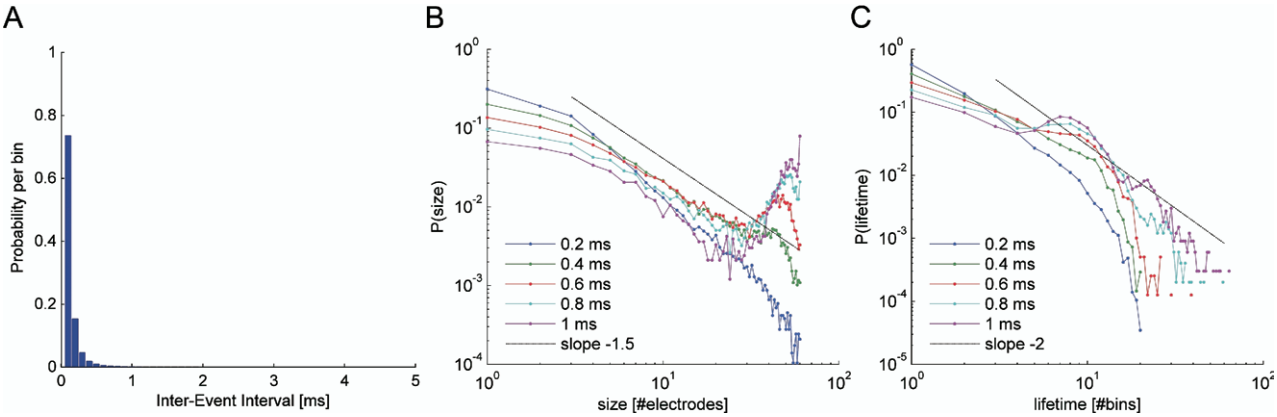

Fig. 10. The network model compares favorably with experimental data, both in terms of signals' time scale (i.e. IEI distribution) and avalanche dynamics. (A) IEI distribution for the model reproducing the spontaneous condition. (B, C) Avalanche size and lifetime distributions for the same network model, computed with increasing bin widths (0.2-0.4-0.6-0.8-1 ms) as in Fig. 3.

The emulation of chemical manipulations by means of ACh and BIC is also reported in Fig. 11A–C. In the first case (ACh, red line), the network activity is ruled by random and isolated spikes and a subcritical behavior appears (cf. also Fig. 9A). Conversely, by reducing all the inhibitory connections to mimic the effect of BIC (i.e. 10% of the original value) a supercritical behavior is observed (cf. Fig. 11A–C, blue line, and Fig. 9B).

The simulated neuronal network dynamics was also characterized by means of CI_0 and percentage of random spikes, as done for the experimental data. Fig. 11E and 11F shows the box plots of the histograms of CI_0 and percentage of random spiking activity for all the three simulated conditions (i.e. spontaneous activity, ACh and BIC addition). The three distributions are statistically different, as confirmed by the Kruskal-Wallis statistical test

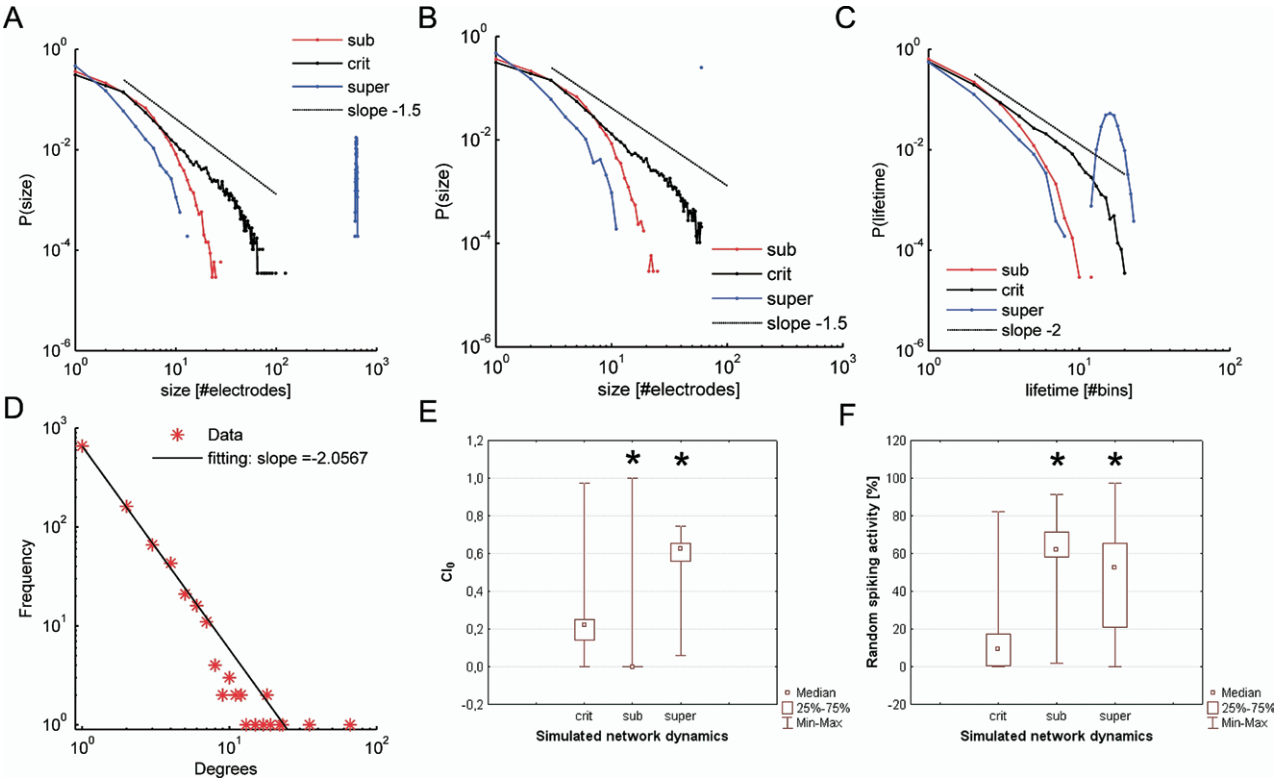

Fig. 11. The simulated model is capable of reproducing both avalanche dynamics and global activity features in different experimental conditions. (A–C) Avalanche size and lifetime distributions (A, size definition 1; B, size definition 2; C, lifetime) coming from the simulation of a large scale neuronal network in three different conditions, i.e. spontaneous activity (black line), ACh (red line) and BIC addition (blue line). Bin width=0.2 ms. (D) Probability distribution of the degree of connectivity in the simulated network. (E, F) Box plots of the CI_0 histogram (E) and the percentage of random spiking activity histogram (F), for the same three aforementioned conditions. Stars indicate statistically significant differences with respect to the critical condition.

(ANOVA for ranks, Kruskal-Wallis test: CI_0, H (N=180)= 116.521, $P \leq 0.001$; percentage of random spiking activity, H (N=70)=12.494, $P \leq 0.05$).

The modeling results show the same qualitative trend as the experimental data, confirming that a supercritical state is typical of cultures with a high CI_0 coefficient, whereas subcritical behavior is synonymous of random and desynchronized activity.

Thus, we demonstrated that a critical behavior, being intrinsic of a specific network topology, can be disrupted by changing the strengths of synaptic connections or the level of neuron excitability.

DISCUSSION

In order to investigate the properties of self-organization and intrinsic dynamics in cultured cortical networks, we extensively analyzed the spontaneous electrophysiological activity during development. We also introduced specific chemical treatments and developed a computational model to better elucidate the universal mechanisms that sustain criticality, correlating the appearance of critical states with bursting behavior and cross-correlation based analysis. Three main conclusions can be drawn from the analysis of the experimental observations. First: neuronal avalanches, originally found in acute and organotypic slices, are also found in dissociated cortical cultures. The time scale of the phenomenon is different as it is referred to spiking activity and not to LFPs (as for slices). Second: the fate of some cultures during development is to reach a critical state. In general, when cell cultures reach a mature state, they tend to fall into one preferred state (critical, subcritical or supercritical). Third: the three states are associated with a particular bursting pattern and degree of synchronization of the network. This was demonstrated through bath application of ACh and BIC and with the help of the developed computational model. Finally, simulated results support the plausibility of a scale-free network topology underlying the critical state.

Neuronal avalanches as a universal mechanism of activity propagation

Since neuronal avalanches were detected in rat somatosensory cortical slices cultured over MEAs (Beggs and Plenz, 2003, 2004), many studies were reported in the literature about the presence of these complex spatio-temporal patterns of activity in different experimental frameworks (Bédard et al., 2006; Stewart and Plenz, 2006), as well as in modeling studies (Abbott and Rohrkemper, 2007; Kinouchi and Copelli, 2006; Levina et al., 2007; Teramae and Fukai, 2007) in order to get insight into the mechanisms that underlie this phenomenon.

A recent review (Plenz and Thiagarajan, 2007) summarizes up-to-date experimental results and classes of computational models which reproduce this kind of dynamics: according to these studies, neuronal avalanches could represent a strong candidate for the representation of cell assemblies in the cortex, having some implications in efficient information coding (Kinouchi and Copelli, 2006) and transmission (Haldeman and Beggs, 2005).

Networks of dissociated neurons coupled to MEAs represent a powerful experimental model in which the presence of neuronal avalanches has not yet been fully investigated. As neurons can freely self-organize without any constraint, forming a functional network whose spontaneous activity can exhibit recurrent patterns of activity (Wagenaar et al., 2006a; Rolston et al., 2007), it is particularly interesting to study whether they are subjected to the same scale-free organization of activity and whether they can reproduce neuronal avalanches.

In a recent report, Mazzoni et al. (2007) also described possible critical behaviors in randomly cultured hippocampal neurons. Although it is not fully clear how they define the parameters to verify the presence of neuronal avalanches, the reported data analysis is obtained by purely analyzing bursting behavior and not accounting for actual sequences of consecutive neuronal activations. The same approach has been recently used in another report (Madhavan et al., 2007). In our work, we derived the criterion for detecting avalanches from the same definition given in their original paper by Beggs and Plenz (2003) for slice cultures and we only adapted the parameters (i.e. time bin of 0.2 ms) to the spiking activity. In this framework this is, to the best of our knowledge, the first time that a critical behavior is demonstrated in cultured networks at the spiking level, and that quantitative and detailed analysis are reported.

As underlined in the Results section, using a time window of 0.2 ms to bin our data, neuronal avalanche size and lifetime distributions appear to follow a linear relationship in bi-logarithmic scale. This is an evidence of self-organized criticality that we found in some cultures at a mature stage of development supporting the idea that this behavior is a universal mechanism that is spontaneously implemented in many neuronal systems. Additionally, it is further evidence that avalanche behavior is the general dynamics that applies at different time scales and reflects different hierarchical levels of organization.

Our results also suggest that cultures of dissociated neurons are capable of reproducing network dynamic behaviors that resemble those found in other *in vitro* preparations in which the architecture is partly maintained (i.e. cultured and acute slices).

Critical states during development

Analyzing different cultures at several ages, we observed all the three possible avalanche distributions, namely subcritical, critical and supercritical.

During the first 3 weeks *in vitro*, avalanche distribution follows a subcritical trend: until 21 DIV, activity is mainly formed of poorly correlated spikes and bursts that originate many little avalanches and few big avalanches. After 21 DIV, the cross-correlation among different electrodes' activity markedly increases, as well as the burst number and the MBR (Chiappalone et al., 2006a): this leads to a higher number of avalanches recorded per minute and to different avalanche distributions.

Despite that cultures come from the same neuronal preparation, their development is free of predefined constraints: this implies that every network can be substantially different from the others, as neurons grow randomly, and we do not know a priori which is the underlying connectivity. Therefore, it is not surprising that not all cultures self-organize and reach a critical state: the variability we usually observe in other parameters which describe the electrical activity of cultured dissociated neurons reflects on the avalanche distribution. Nevertheless, all the cultures are able to reproduce neuronal avalanches and some of them approach criticality, demonstrating that they preserve some properties of self-organization characteristic of *in vivo*–formed cell assemblies (Petermann et al., 2006).

To summarize, as soon as cell cultures reach a mature state, they tend to fall into one preferred state (critical, subcritical or supercritical), from which little deviation is possible. Studying which factors influence the formation of critical networks is beyond the aim of this work and will be object of future investigation. Certainly, it would be interesting to compare avalanche analysis results with connectivity maps extracted from the same recordings, in order to correlate the network graph with the avalanche behavior.

Role and significance of neuronal avalanches

Neuronal avalanches in cultures of neurons are associated with other parameters describing spiking and bursting dynamics, mainly the degree of synchronization of bursts among different channels and the proportion between spiking and bursting activity.

Supercritical behavior is associated with a high degree of synchronization of bursts among all the electrodes, whereas subcritical behavior is related to low synchronization and high percentage of non-clustered activity. Therefore, the critical state is achieved when spontaneous electrical activity is composed of both medium-synchronized network bursts (van Pelt et al., 2004b) and a very small amount of random spikes. When the activity is highly synchronized, all neurons fire together and frequently originate avalanches involving the whole network: in this case, the distribution of avalanche sizes is bimodal, as in cortical slices after treatment with picrotoxin (Beggs and Plenz, 2003).

The same, as discussed, spontaneously applies for some cultures or after treatment with BIC (mimicking exactly what is happening in cortical slices).

Conversely, when the electrical activity is poorly correlated, each electrode fires independently, and global avalanches occur with a lower probability. A medium-level synchronization usually corresponds to a nearly critical state, suggesting that criticality is strictly linked to the degree of connectivity, both in anatomical and functional terms (Sporns et al., 2004). The relation among avalanche dynamics, synchronization and percentage of random spiking activity was confirmed by chemical stimulation results and simple neuronal network models, which are directly inspired to our cultures and reproduce the different experimental conditions.

Therefore, in this framework, criticality is related to the amount of variability present in the network, and so to entropy, according to the degree of correlation among different electrodes. Thus, a condition for the self-organized criticality to be reached seems to be a degree of connectivity able to both ensure an appropriate level of synchronization and an efficient local propagation of signals through the network, avoiding the saturation of the network itself each time a single unit is activated. From the developed model we could assume that a scale-free network topology is a good candidate to support such critical behavior.

Such a system would be able to optimize information coding and also information transmission: for these reasons, the next step will be to combine this study with the application of information theory to the activity of our cultures.

The dynamic process at the base of neuronal avalanches' formation deserves further investigation: several models have been proposed (see Plenz and Thiagarajan (2007) for an exhaustive review), but so far it is still not clear which one best explains the appearance of a scale-free distribution in the neural activity recorded from both *in vivo* and *in vitro* systems. Beggs and Plenz (2003) were inclined to believe that a critical branching process underlies this phenomenon in cortical slices, but this is only one of the possible explanations, although they estimated the value of the branching parameter close to 1. The aforementioned review paper (Plenz and Thiagarajan, 2007) illustrates some objections to this interpretation.

Our choice of using shorter time windows to bin the data (i.e. 0.2 ms) relied on average IEI values and on considerations about spikes' timescale, as well as on measures of the propagation velocity (~300 mm/s) in cultures of dissociated neurons (Jacobi and Moses, 2007). We are aware of the fact that such a high value for the propagation velocity of neural activity is incompatible with the hypothesis of the feedforward signal's conduction on polysynaptic pathways, as it would be if we considered a "simple" branching process. Consequently, we hypothesized that the collective network activity (i.e. synchronized network bursts) showed by dense cultures of dissociated neurons is composed of both almost simultaneous activations of multiple sites and a local signal propagation spreading from the sites themselves. Thus, the choice of a small time bin is necessary to catch the dynamics of cultures at a subtler level. These considerations were confirmed through the application of the shuffling procedures to the experimental data.

At this stage, any consideration about the origin of avalanches will be a mere speculation, but we think that this work highlights the fact that different mechanisms other than critical branching process may underlie the formation of neuronal avalanches (e.g. involving also complementary phenomena, like synchronization).

Of course, the underlying mechanism of avalanches deserves further investigation to be fully understood, through both an experimental and modeling approach.

CONCLUSION

In summary, cultures of dissociated cortical neurons developing *in vitro* are capable of displaying spontaneous spiking activity which is organized in the form of neuronal avalanches; some cultures present a critical distribution of avalanche sizes and lifetimes at a mature age, supporting the hypothesis that neurons preserve the capability of self-organizing in an effective system even *in vitro*. We have demonstrated the significance of the results by comparing distributions obtained from actual data and random-shuffled data and we related it to the global activity presented by the network, in particular to the degree of burstiness and synchronization. Finally, this relation has been confirmed by appropriate chemical stimulation experiments and computational models.

Acknowledgments—We are grateful to Dr. Brunella Tedesco for the preparation and maintenance of cell cultures. We wish also thank Prof. Fabio Benfenati for useful discussions.

REFERENCES

Abbott LF, Rohrkemper (2007) A simple growth model constructs critical avalanche networks. Prog Brain Res 65:13–19.

Araque A, Parpura V, Sanzgiri RP, Haydon PG (1999) Tripartite synapses: glia, the unacknowledged partner. Trends Neurosci 22:208–215.

Bak P (1996) How nature works: the science of self-organized criticality. New York: Copernicus Press.

Bak P, Tang C, Wiesenfeld K (1987) Self-organized criticality: an explanation of 1/f noise. Phys Rev Lett 59:381–384.

Bak P, Tang C, Wiesenfeld K (1988) Self-organized criticality. Phys Rev A 38:364–374.

Barabasi A-L, Albert R (1999) Emergence of scaling in random networks. Science 286:509–512.

Bédard C, Kroger H, Destexhe A (2006) Does the 1/f frequency scaling of brain signals reflect self-organized critical states? Phys Rev Lett 97:118102.

Beggs JM, Plenz D (2003) Neuronal avalanches in neocortical circuits. J Neurosci 23:11167–11177.

Beggs JM, Plenz D (2004) Neuronal avalanches are diverse and precise activity patterns that are stable for many hours in cortical slice cultures. J Neurosci 24:5216–5229.

Bonifazi P, Ruaro ME, Torre V (2005) Statistical properties of information processing in neuronal networks. Eur J Neurosci 22: 2953–2964.

Braitenberg V, Schultz A (1991) Anatomy of the cortex: statistics and geometry. Berlin: Springer-Verlag.

Brewer GJ (1997) Isolation and culture of adult rat hippocampal neurons. J Neurosci Methods 71:143–155.

Brewer GJ, Torricelli JR, Evege EK, Price PJ (1993) Optimized survival of hippocampal neurons in B27-supplemented neurobasal, a new serum-free medium combination. J Neurosci Res 35: 567–576.

Buchmann J, Schulten K (1987) Influence of noise on the function of a "physiological" neural network. Biol Cyber 56:313–327.

Chebib M, Johnston GAR (1999) The "ABC" of GABA receptors: a brief overview. Clin Exp Pharmacol Phys 26:937–940.

Chialvo DR (2004) Critical brain networks. Physica A 340:756–765.

Chialvo DR (2006) The brain near the edge. In: Cooperative behavior in neural systems: ninth grade lectures, vol. 887 (Marro J et al., eds), pp 1–12. Granada, Spain: AIP Proceedings.

Chiappalone M, Bove M, Vato A, Tedesco M, Martinoia S (2006a) Dissociated cortical networks show spontaneously correlated activity patterns during in vitro development. Brain Res 1093:41–53.

Chiappalone M, Massobrio P, Tedesco MT, Martinoia S (2006b) Stimulus-induced distributed synaptic changes in networks of cortical neurons. In: MEA meeting 2006, Vol. proceedings MEA meeting 2006 (Stett A, ed), pp 32–33. Reutlingen: BIOPRO.

Chiappalone M, Novellino A, Vajda I, Vato A, Martinoia S, van Pelt J (2005) Burst detection algorithms for the analysis of spatio-temporal patterns in cortical networks of neurons. Neurocomputing 65–66:653–662.

Chiappalone M, Vato A, Berdondini L, Koudelka M, Martinoia S (2007) Network dynamics and synchronous activity in cultured cortical neurons. Int J Neural Syst 17:87–103.

Chiappalone M, Vato A, Tedesco M, Marcoli M, Davide FA, Martinoia S (2003) Networks of neurons coupled to microelectrode arrays: a neuronal sensory system for pharmacological applications. Biosens Bioelectron 18:627–634.

Corral A, Perez CJ, Diaz-Guilera A, Arenas A (1995) Self-organized criticality and synchronization in a lattice model of integrate-and-fire oscillators. Phys Rev Lett 74:118–121.

Cozzi L, D'Angelo P, Sanguineti V (2006) Encoding of time-varying stimuli in population of cultured neurons. Biol Cyber 94:335–349.

Dayan P, Abbott LF (2001) Theoretical neuroscience: computational and mathematical modeling of neural systems. Cambridge: MIT Press.

Eguiluz VM, Chialvo DR, Cecchi GA, Baliki M, Apkarian AV (2005) Scale-free brain functional networks. Phys Rev Lett 94:018102.

Eytan D, Marom S (2006) Dynamics and effective topology underlying synchronization in networks of cortical neurons. J Neurosci 26: 8465–8476.

Eytan D, Minerbi A, Ziv N, Marom S (2004) Dopamine-induced dispersion of correlations between action potentials in networks of cortical neurons. J Neurophysiol 92:1817–1824.

Fransen E, Tahvildari B, Egorov AV, Hasselmo ME, Alonso A (2006) Mechanism of graded persistent cellular activity of entorhinal cortex layer V neurons. Neuron 49:735–746.

Freeman WJ (1975) Mass action in the nervous system. New York: Academic Press.

Gramowski A, Jugelt K, Weiss DG, Gross GW (2004) Substance identification by quantitative characterization of oscillatory activity in murine spinal cord networks on microelectrode arrays. Eur J Neurosci 19:2815–2825.

Gross GW, Azzazy HME, Wu MC, Rhodes BK (1995) The use of neuronal networks on multielectrode arrays as biosensors. Biosens Bioelectron 10:553–567.

Haj-Dahmane S, Andrade R (1996) Muscarinic activation of a voltage-dependent cation nonselective current in rat association cortex. J Neurosci 16:3848–3861.

Haldeman C, Beggs J (2005) Critical branching captures activity in living neural networks and maximizes the number of metastable states. Phys Rev Lett 94:058101.

Hasselmo ME (2006) The role of acetylcholine in learning and memory. Curr Opin Neurobiol 16:710–715.

Hsu D, Tang A, Hsu M, Beggs JM (2007) Simple spontaneously active Hebbian learning model: Homeostasis of activity and connectivity, and consequences for learning and epileptogenesis. Phys Rev E 76:041909.

Izhikevich EM (2003) Simple model of spiking neurons. IEEE Trans Neural Netw 6:1569–1572.

Izhikevich EM (2004) Which model to use for cortical spiking neurons? IEEE Trans Neural Netw 15:1063–1070.

Jacobi S, Moses E (2007) Variability and corresponding amplitude-velocity relation of activity propagating in one-dimensional neural cultures. J Neurophysiol 97:3597–3606.

Jimbo Y, Tateno Y, Robinson HPC (1999) Simultaneous induction of pathway-specific potentiation and depression in networks of cortical neurons. Biophys J 76:670–678.

Keefer EW, Gramowski, Gross GW (2001) NMDA receptor-dependent periodic oscillations in cultured spinal cord networks. J Neurophysiol 86:3030–3042.

Kinouchi O, Copelli M (2006) Optimal dynamical range of excitable networks at criticality. Nat Phys 2:348–352.
Klink R, Alonso A (1997) Muscarinic modulation of the oscillatory and repetitive firing properties of entorhinal cortex layer II neurons. J Neurophysiol 77:1813–1828.
Levina A, Ernst U, Herrman JM (2007) Criticality of avalanche dynamics in adaptive recurrent networks. Neurocomputing 70:1877–1881.
Lin Y-C, Hung Z-H, Jan I-S, Yeh C-C, Wu H-J, Chou Y-C, Chang Y-C (2002) Development of excitatory synapses in cultured neurons dissociated from the cortices of rat embryos and rat pups at birth. J Neurosci Res 67:484–493.
Madhavan R, Chao ZC, Potter SM (2007) Plasticity of recurring spatiotemporal activity patterns in cortical networks. Phys Biol 4: 181–193.
Marom S, Shahaf G (2002) Development, learning and memory in large random networks of cortical neurons: lessons beyond anatomy. Q Rev Biophys 35:63–87.
Massobrio P, Massobrio G, Martinoia S (2007) Multi-program approach for simulating recorded extracellular signals generated by neurons coupled to microelectrode arrays. Neurocomputing 70:2467–2476.
Mazzoni A, Broccard FD, Garcia-Perez E, Bonifazi P, Ruaro ME, Torre V (2007) On the dynamics of the spontaneous activity in neuronal networks. PLoS ONE 2:e439.
Nedergaard M (1994) Direct signaling from astrocytes to neurons in cultures of mammalian brain cells. Science 263:1768–1771.
Opitz T, De Lima AD, Voigt T (2002) Spontaneous development of synchronous oscillatory activity during maturation of cortical networks in vitro. J Neurophysiol 88:2196–2206.
Park K, Lai Y-C, Ye N (2005) Self-organized scale-free networks. Phys Rev E 72:261311–261315.
Perkel DH, Gerstein GL, Moore GP (1967) Neuronal spike train and stochastic point processes I. The single spike train. Biophys J 7:391–418.
Petermann T, Lebedev MA, Nicolelis MAL, Plenz D (2006) Neuronal avalanches in vivo. In: Society for Neuroscience Atlanta, USA.
Pfrieger FW, Barres BA (1997) Synaptic efficacy enhanced by glial cells in vitro. Science 277:1684–1687.
Plenz D, Thiagarajan TC (2007) The organizing principles of neuronal avalanches: cell assemblies in the cortex? Trends Neurosci 30:101–110.
Robinson HPC, Kawahara M, Jimbo Y, Torimitsu K, Kuroda Y, Kawana A (1993) Periodic synchronized bursting in intracellular calcium transients elicited by low magnesium in cultured cortical neurons. J Neurophysiol 70:1606–1616.
Rolston JD, Wagenaar DA, Potter SM (2007) Precisely timed spatiotemporal patterns of neural activity in dissociated cortical cultures. Neuroscience 148:294–303.
Ruaro ME, Bonifazi P, Torre V (2005) Toward the neurocomputer: image processing and pattern recognition with neuronal cultures. IEEE Trans Biomed Eng 52:371–383.
Sporns O, Chialvo DR, Kaiser M, Hilgetag CC (2004) Organization, development and function of complex brain networks. Trends Cogn Sci 8:418–425.
Stewart CV, Plenz D (2006) Inverted-U profile of dopamine-NMDA-mediated spontaneous avalanche recurrence in superficial layers of rat prefrontal cortex. J Neurosci 26:8148–8159.
Streit J, Tscherter A, Heuschkel MO, Renaud P (2001) The generation of rhythmic activity in dissociated cultures of rat spinal cord. Eur J Neurosci 14:191–202.
Tateno T, Jimbo Y (1999) Activity-dependent enhancement in the reliability of correlated spike timings in cultured cortical neurons. Biol Cybern 80:45–55.
Teramae J-N, Fukai T (2007) Local cortical circuit model inferred from power-law distributed neuronal avalanches. J Comput Neurosci 22:301–312.
van Ooyen A, van Pelt J (1996) Complex periodic behaviour in a neuronal network model with activity-dependent neurite outgrowth. J Theor Biol 179:229–242.
van Pelt J, Corner MA, Wolters PS, Rutten WLC, Ramakers GJA (2004a) Long-term stability and developmental changes in spontaneous network burst firing patterns in dissociated rat cerebral cortex cell cultures on multi-electrode arrays. Neurosci Lett 361:86–89.
van Pelt J, Wolters PS, Corner MA, Rutten WLC, Ramakers GJA (2004b) Long-term characterization of firing dynamics of spontaneous bursts in cultured neural networks. IEEE Trans Biomed Eng 51:2051–2062.
van Pelt J, Vajda I, Wolters PS, Corner MA, Ramakers GJA (2005) Dynamics and plasticity in developing neural networks in vitro. Prog Brain Res 147:171–188.
Wagenaar DA, Nadasdy Z, Potter SM (2006a) Persistent dynamic attractors in activity patterns of cultured neuronal networks. Phys Rev E 73:051907.
Wagenaar DA, Pine J, Potter SM (2006b) An extremely rich repertoire of bursting patterns during the development of cortical cultures. BMC Neurosci 7:11.
Zapperi S, Baekgaard LK, Stanley HE (1995) Self-organized branching process: mean-field theory for avalanches. Phys Rev Lett 75:4071–4074.

(Accepted 12 March 2008)
(Available online 29 March 2008)